

## 3-2-4 Relationship between Equatorial Electrojet Variation and Spread- $F$ Occurrence

UEMOTO Jyunpei, MARUYAMA Takashi, SAITO Susumu, ISHII Mamoru, and YOSHIMURA Reiko

Equatorial spread- $F$  (ESF) is electron density irregularity occurring in the post-sunset equatorial  $F$ -region ionosphere that causes interruption and degradation to various satellite communication and navigation systems. It has been clarified that various physical parameters and processes control ESF occurrence and development. In addition to such controlling factors, recent observations suggest a relationship between ESF occurrence and equatorial electrojet (EEJ) strength. We discuss the recent observational results including a data analysis of SEALION observations and possible mechanisms of the relationship between ESF and EEJ.

### **Keywords**

Equatorial spread- $F$ , Equatorial electrojet, Pre-reversal enhancement

### **1 Introduction**

It is well known that an electron density irregularity called equatorial spread- $F$  (ESF) often occurs in the post sunset equatorial  $F$ -region ionosphere. This phenomenon occurs at the bottom side  $F$ -region and develops nonlinearly with time; ESF may spread in the latitudinal direction while rising explosively, and sometimes even reaches the southern part of Japan [1]. The scale of such a nonlinearly developed irregularity varies widely from several centimeters to hundreds of kilometers, thereby adversely affecting the radio waves of various frequency bands. Against this background and with advanced technologies now being used for radio waves between the ground and satellites (as typified by GPS positioning) to provide familiar services as part of our daily lives, the importance of predicting the generation of ESF that may disturb radio propagation is globally recognized. The physical quantities and physical processes concerning the generation of ESF are known to vary widely. This special issue describes various physical processes related to the development

of ESF (*e.g.*, Reference [2]). This paper describes the results derived from analyzing SEALION data as pertaining to the relationship between the equatorial electrojet (EEJ) strength and ESF, which have been better clarified by observational studies in recent years.

### **2 Outline of EEJ, PRE and ESF**

#### **2.1 Equatorial electrojet**

The vertical  $\mathbf{E} \times \mathbf{B}$  drift of plasma caused by the horizontal and northward magnetic field line and east-west electric field largely affects the structure and dynamics of the equatorial ionosphere. The  $\mathbf{E} \times \mathbf{B}$  drift in the  $F$ -region is basically upward during the daytime. The eastward electric field that causes this upward  $\mathbf{E} \times \mathbf{B}$  drift is the electric field driven by the  $E$ -region dynamo as mapped into the  $F$ -region via magnetic field lines considered to be an equi-potential. The east-west current driven in the  $E$ -region at the same time as this dynamo electric field is intensified by the Cowling effect near the magnetic equator (within  $\pm 3^\circ$ ). Figure 1 shows a schematic diagram of the Cowling effect.

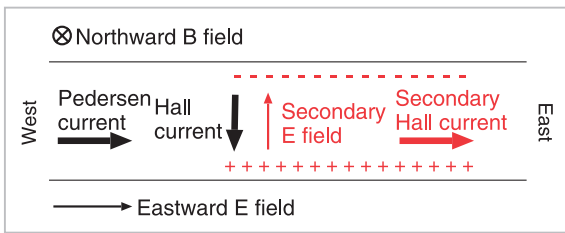


**Fig.1** Schematic diagram of the Cowling effect

The Hall current indicated by the black arrow generates charge separation in the vertical direction. An upward secondary electric field occurs in the direction that resolves this separation, and drives the secondary eastward Hall current.

This figure shows a view of the magnetic equator from the south, with the magnetic field oriented toward this paper surface. When an eastward electric field exists, a Pedersen current will flow in the same direction as the electric field, while a Hall current will flow in a direction perpendicular to the electric field and magnetic field. This Hall current causes the vertical charge separation, resulting in an upward electric polarization field to resolve this charge separation. A secondary Hall current due to this electric polarization field will flow eastward which is the same direction as the Pedersen current generated by the eastward electric field, thereby intensifying the eastward current. EEJ refers to the current intensified by this Cowling effect [3]. The eastward EEJ is normally prominent during the daytime, while a westward EEJ called counter EEJ (CEJ) is sometimes observed. Since the EEJ causes large variations in the horizontal component of the magnetic field many studies based on analyzing magnetometer data have been conducted (see Reference [4]). When evaluating the EEJ by using the horizontal component of the magnetic field, the global variations brought about by currents flowing in the magnetosphere (such as a ring current) must be removed. Often used for that purpose is a method where the residual between the horizontal components near the magnetic equator and those from the magnetic low-latitude region slightly away from the magnetic

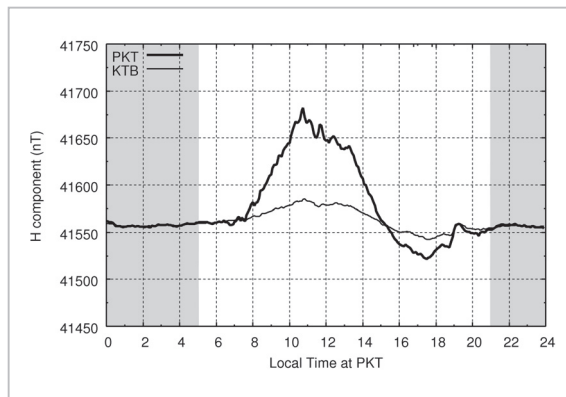


**Fig.2** An example of an EEJ evaluation method that uses the horizontal component of the magnetic field

The thick line indicates the horizontal component obtained near the magnetic equator; the thin line indicates that in the magnetic low-latitude region adjusted to minimize the difference from that observed near the magnetic equator during the period from 21 to 05 LT. The horizontal components near the magnetic equator and at low-latitude are the values observed at Phuket, Thailand (8.1°N, 98.3°E, 0.1°N magnetic latitude), and at Kototabang, Indonesia (0.2°S, 100.3°E, 10.0°S magnetic latitude) on April 12, 2008, respectively. The portion enclosed by both lines represents changes in the horizontal component stemming from the EEJ. The CEJ occurred around the period from 15 to 19 LT.

equator are regarded as a proxy of EEJ intensity. Figure 2 shows an example of a method of evaluating the EEJ strength that uses the horizontal component of the magnetic field.

The thick and thin lines represent local time variations in the horizontal components near the magnetic equator and those in the magnetic low-latitude region slightly away from the magnetic equator, respectively. The portion enclosed by both lines represents changes of the horizontal component stemming from the EEJ.

## 2.2 Pre-reversal enhancement

The upward  $\mathbf{E} \times \mathbf{B}$  drift during the daytime driven by the  $E$ -region dynamo becomes downward during the nighttime. The direction of this drift is reversed at around post-sunset, but the upward  $\mathbf{E} \times \mathbf{B}$  drift is well known to

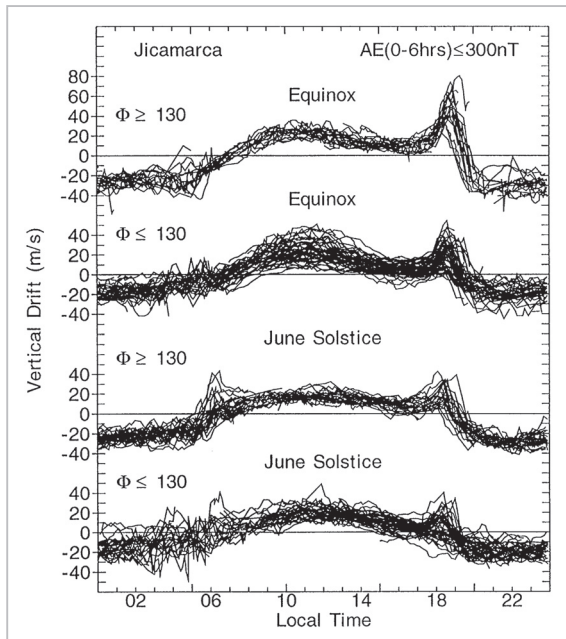


**Fig.3** Vertical drift in the F-region observed using the IS radar in Jicamarca, Peru ( $11.9^{\circ}\text{S}$ ,  $283.2^{\circ}\text{E}$ ,  $1.0^{\circ}$  dip latitude) [7].

The figure shows the upward drift has increased (PRE) before the direction of drift is reversed at around 18 LT.

often increase before the reversing. This phenomenon is called pre-reversal enhancement (PRE) (Fig. 3).

The intensity of PRE can be derived from an IS radar, in-situ ion drift observation, ionosonde observation, or other monitoring methods. The IS radar can observe PRE most accurately, but few IS radars are deployed in the equatorial region. Another method often used is deriving PRE from the altitudinal variation of the bottom side F-layer ( $h'F$ ) as obtained from ionosonde observation. It should be noted that  $h'F$  generally differs from the actual altitude. This is because ionospheric plasma makes the group velocity of radio waves slower than that of radio waves in a vacuum. However, during the nighttime, the electron density below the bottom side F-region declines considerably, thereby reducing the difference between the apparent altitude and the actual one. Reference [5] reported that the local time variation of  $h'F$  can be considered that of  $\mathbf{E} \times \mathbf{B}$  drift during the nighttime. Observations made to date have clarified that

the characteristics of PRE depend on solar activity, the season, geographical longitude, and geomagnetic activity (see References [6] and [7]), but PRE is also known to show considerable day-to-day variations that have yet to be predicted. As described below, PRE plays an important role in the generation and development of ESF, making the elucidation of day-to-day variations very important. On the other hand, studies on the generation mechanism of PRE are being conducted by numerical calculations, and have clarified the source of PRE as being the F-region dynamo (see References [8] and [9]). However, the physical process connecting the F-region dynamo and PRE is not simple. The generation mechanisms of PRE proposed thus far are the mechanism whereby sudden vertical electric field changes due to the F-region dynamo generate a horizontal electric field to satisfy the curl-free conditions, the mechanism whereby a negative charge is accumulated in the low-latitude E-region as described in Reference [11], and the mechanism whereby the dispersion current of EEJ and the vertical current generated by the F-region dynamo are connected as described in Reference [12]. Although Reference [8] compared these three mechanisms according to numerical calculations and reported that the mechanism described in Reference [10] is essential and the other mechanisms are auxiliary, all these mechanisms have not actually been sufficiently verified through observation.

### 2.3 Equatorial spread-F

It has been clarified that the initial development stage of ESF that occurs near sunset can be explained by the Rayleigh-Taylor instability (see Reference [13]). Figure 4 is a schematic diagram of the Rayleigh-Taylor instability in the equatorial ionospheric F-region.

In the altitude region below the F2 peak, the plasma density is higher at higher altitudes. Due to the effects of atmospheric gravity waves and other factors, density fluctuation in east-west directions are formed and, when

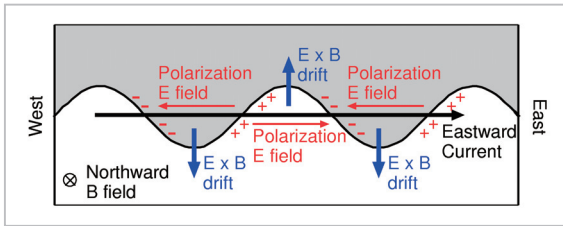


**Fig.4** Schematic diagram of Rayleigh-Taylor instability

When an eastward current as indicated by the black arrow flows through a westward-eastward density fluctuation, a charge separation occurs, resulting in an electric polarization field as indicated by the red arrow. The direction of the  $\mathbf{E} \times \mathbf{B}$  drift (blue arrow) stemming from this electric polarization field faces downward in the portion with high electron density (gray) and upward in the portion with low electron density, resulting in a further increase in the amplitude of density fluctuations.

an eastward current flows, a polarized charge occurs as shown in Fig. 4. The direction of the  $\mathbf{E} \times \mathbf{B}$  drift of the polarized electric field due to this polarized charge is upward in the low-density region and downward in the high-density region, thereby further increasing the amplitude of density fluctuations and resulting in growing instability. Things are actually not as simple as depicted in Fig. 4, and the various physical quantities and physical processes are related to the growth of ESF as stated in Reference [14], making the generation mechanism of ESF very complex. One complicating factor is that, due to the very high conductivity along the magnetic field lines, the integral values of physical quantities along the magnetic field lines must be taken into account when considering the linear growth rate of the Rayleigh-Taylor instability. For example, the effects inhibiting ESF growth due to trans-equatorial neutral winds in the magnetic meridional plane as stated in Reference [2] cannot be explained by Fig. 4 where electric connection via a magnetic field line is not considered. Another complicating factor is the effect where a change in one physical quantity changes another physical quantity, thereby indirectly affecting the growth rate of ESF.

For example, the eastward electric field intensifies the eastward current as shown in Fig. 4, thereby promoting the growth of ESF, while simultaneously raising the altitude of the ionosphere due to the upward  $\mathbf{E} \times \mathbf{B}$  drift, and thus indirectly exercising a positive influence on the growth of instability through reducing the ion-neutral collision frequency.

Although the growth rate of ESF is governed by various physical quantities and complex physical processes in this way, PRE is the most influential (albeit not with a complete one-to-one correspondence) physical quantity, as reported in previous studies (*e.g.*, in Reference [14]). The prediction of PRE intensity can therefore be considered one of the most important steps toward predicting the generation and growth of ESF.

### 3 Relationship between EEJ, PRE, and ESF

#### 3.1 EEJ during the daytime

Based on the analysis of observational data in recent years, the relationship between the EEJ strength during the daytime on one hand, and PRE intensity near sunset and ESF generation on the other, has been revealed (*e.g.*, References [15] and [16]). The relationship with the EEJ strength during the daytime has important significance for predicting the generation of ESF. This is because the EEJ strength during the daytime can be observed prior to PRE near sunset and prior to the generation of ESF after sunset, and therefore useful in predicting the generation of ESF. Reference [15] states that an analysis of scintillation data of the VHF band and magnetometer data obtained in India from September to December 1989 proved that a positive correlation exists between the EEJ strength at 11 LT and the development of ESF after sunset (Fig. 5).

Reference [16] also analyzed magnetometer data and ionosonde data obtained in India from 2001 to March 2005, and states that a good correlation exists between the integral value of the EEJ strength during the period from 07 to 17 LT and the occurrence or non-

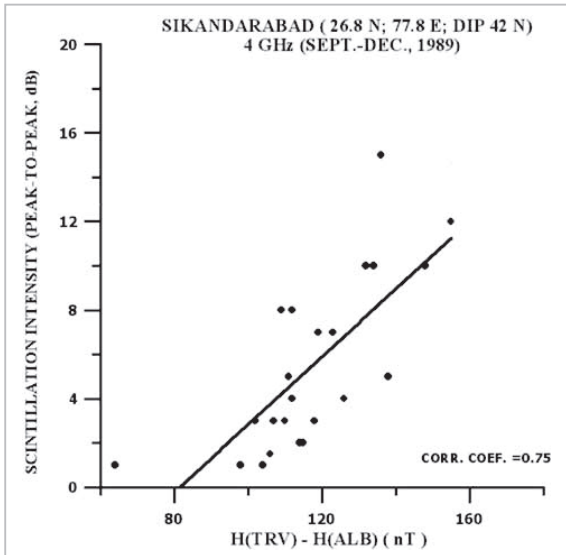


**Fig.5** Correlation diagram between scintillation intensity with a frequency of 4 GHz after sunset and EEJ during the daytime as observed from September to December 1989 [15]

Scintillation intensity was observed at SikanDarabad, India (26.8°N, 77.8°E, 20.8°N magnetic latitude). The EEJ strength was derived from magnetometer data obtained in Trivandrum, India (8.5°N, 76.8°E, 0.3°N magnetic latitude), and in Alibag, India (18.6°N, 72.8°E, 13.4°N magnetic latitude).

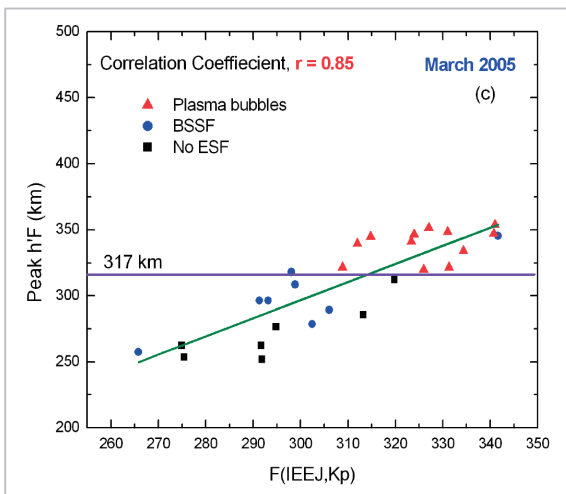


**Fig.6** Correlation diagram between  $h'F$  near sunset derived from an ionosonde at Trivandrum and the time integral value of the EEJ strength during the daytime in March 2005 [16].

The EEJ strength was derived from magnetometer data obtained in Tirunelveli, India (8.7°N, 77.7°E, 0.6°N magnetic latitude) and in Alibag. Note that  $F(IEEJ, Kp)$  on the x-axis is a function of the EEJ strength and  $Kp$ .

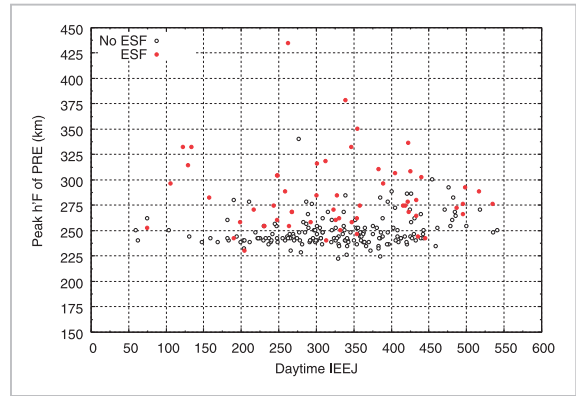


**Fig.7** Correlation diagram between  $h'F$  near sunset and the time integral value of the EEJ strength during the daytime in Southeast Asia during the one-year period from November 2007 to October 2008

Note that  $h'F$  is derived from the ionosonde in Chumphon, Thailand (10.7°N, 99.4°E, 3.3°N magnetic latitude), and the EEJ strength is derived from the magnetometer data obtained in Phuket and Kototabang. The red and white dots indicate the occurrence or non-occurrence of ESF, respectively.

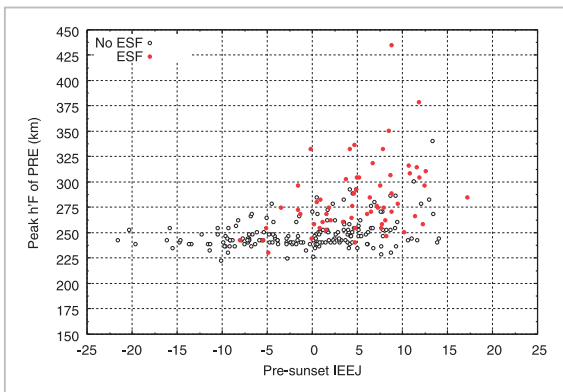
occurrence of ESF (Fig. 6).

In both analyses, comparisons were made with the intensity of PRE derived from  $h'F$  obtained with an ionosonde, and both analyses show a good correlation between the EEJ strength and PRE (Fig. 6). However, these analysis results do not cover all the seasons. Figure 7 shows the data analysis results from SEALION, indicating no such positive correlation through all the seasons, at least in the Southeast Asian region.

### 3.2 EEJ before sunset

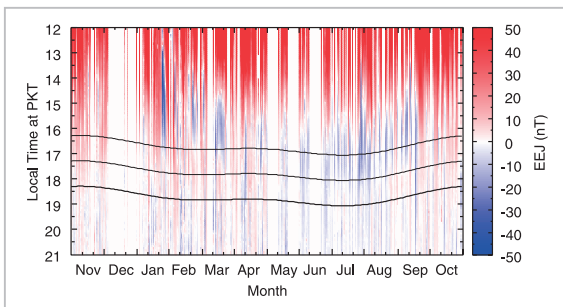
Recent analysis of SEALION data has clarified, on the other hand, that an interesting relationship exists through all the seasons between the time integral value of the EEJ strength one to two hours before sunset and PRE (Fig. 8).

Figure 8 indicates that PRE tends to be inhibited on days when the time integral value of the EEJ strength is small before sunset. Moreover, regarding the occurrence or non-occurrence of ESF, when the integral value of the EEJ strength before sunset is small, the



**Fig.8** Correlation diagram between  $h'F$  near sunset and the time integral value of the EEJ strength one to two hours before sunset in Southeast Asia during the one-year period from November 2007 to October 2008

In time integration, the eastward direction of EEJ is taken as positive.



**Fig.9** Variation of the EEJ strength at Phuket during the one-year period from November 2007 to October 2008

The thick line indicates the sunset time at the  $E$ -region altitude over Phuket; the two thin lines represent the times one to two hours before sunset, respectively.

generation of ESF is inhibited. This inhibition of ESF can be understood as a reasonable result when considering that PRE most affects the Rayleigh-Taylor instability. Conversely, when the time integral value of the EEJ strength before sunset is positive, the relationship between the time integral value of the EEJ strength, intensity of PRE, and occurrence of ESF before sunset shows dispersions and no clear relationship. This is because the intensity of PRE is not necessarily determined by the magnitude of the time integral value of the EEJ strength before sunset. Figure 9 shows

variation of the EEJ strength from 12 to 21 LT during the one-year period from November 2007 to October 2008.

The red portion in the figure indicates that the EEJ is positive (eastward), while the blue portion indicates that the EEJ is negative (westward), meaning that CEJ occurred. From this figure, one can see that there is a high probability that CEJ occurred around 17 LT in the afternoon. This CEJ corresponds to evening CEJ as classified in Reference [17]. One can also see that CEJ frequently occurred in the June solstice season and less frequent in the December solstice season. It can also be seen that the onset time of evening CEJ depends on the season, and occurs at the latest local time during the June solstice season. The thick curve in the figure represents the sunset time at the  $E$ -region altitude (of 100 km); the portions enclosed by the two thin curves indicate one and two hours before sunset, respectively. The portion enclosed by these thin curves represents the integrated range of the EEJ strength before sunset. Comparing the time integrated range of the EEJ strength with the color contours reveals that the time integral value of the EEJ strength before sunset becomes negative, which corresponds to the occurrence of evening CEJ. In considering the results shown in Fig. 8, one can therefore say that PRE is inhibited on days when evening CEJ occurs.

### 3.3 Physical processes connecting EEJ before sunset, PRE near sunset, and ESF after sunset

Figures 8 and 9 indicate that PRE is inhibited on days when the time integral value of the EEJ strength before sunset is negative, that is, when evening CEJ occurred. Moreover, regarding the occurrence or non-occurrence of ESF, one can see that the occurrence of ESF is inhibited on days when the time integral value of the EEJ strength is small. With regard to the inhibited occurrence of ESF, the result can be deemed reasonable when considering that PRE most affects the growth rate of the Rayleigh-Taylor instability, but explaining the

relationship between the time integral value of the EEJ strength before sunset and PRE near sunset is not so easy. There are at least two different physical processes regarding the relationship between the time integral value of the EEJ strength before sunset and PRE as described below.

The first physical process is the connection via the daytime EEJ and vertical current in the *F*-region near sunset. Reference [12] reported by performing a numerical calculation that EEJ would connect to the vertical current caused by the *F*-region dynamo (Fig. 10).

When this connection is established, an eastward current needs to flow in the region where the conductivity is low near sunset. For that reason, Reference [12] states that the *E*-region with the low conductivity entails a need for a strong eastward electric field, and that this eastward electric field intensifies PRE. Reference [18] presents observation results that indicate the presence of a dispersion current of EEJ according to observations of 3-meter irregularities in the *E*-region. Calculations have not been performed to determine PRE concerning the day when evening CEJ occurred. However, on days when evening CEJ occurs, a westward current is considered to flow in the *E*-region near sunset. In that

case, the intensification mechanism of PRE proposed in Reference [12] is not triggered; therefore, the intensity of PRE can be considered inhibited. However, Fig. 8 is the result obtained by comparing the time integral value of the EEJ strength before sunset and PRE after sunset at the same longitude. One should therefore keep in mind that spatial changes are not rigorously observed.

The second physical process is the connection via changes in the distribution of plasma, that is, the distribution of conductivity in the meridional plane due to the electric field of the *E*-region dynamo. The relationship associated with the plasma distribution in the magnetic meridional plane, the intensity of PRE, and the occurrence or non-occurrence of ESF has been widely studied, particularly in India. Reference [15] reports that a positive correlation exists between PRE near sunset and the development of the equatorial anomaly after sunset. Reference [19] presents observations made in India to statistically show that plasma density increases near the crest of the equatorial anomaly and in the latitude zone inside the crest on ESF days (Fig. 11).

Reference [20] compared the beacon TEC and ESF obtained in India, and found that ESF occurs when the equatorial anomaly is symmetric and intense during the period from 16 to 18.75 LT. Moreover, Reference [21] suggests, by performing numerical calculations, the possibility of a relationship existing between the distribution of plasma inside the equatorial anomaly and PRE. It is conceivable that the distribution of plasma inside the equatorial anomaly near sunset is changed by the electric field of the *E*-region dynamo one to two hours before sunset. Hence, Fig. 8 can be considered to represent the relationship between the *E*-region dynamo one to two hours before sunset and PRE via changes in plasma distribution inside the equatorial anomaly.

As stated in Section 2.2, Reference [8] indicates through model calculations that the PRE mechanism via the connection of EEJ and vertical current in the *F*-region proposed by Reference [12] are auxiliary. However, because no

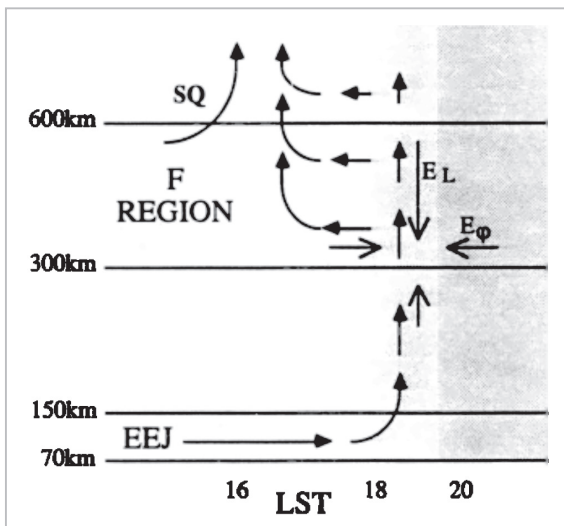


**Fig. 10** Schematic diagram indicating the connection of EEJ during the daytime and vertical current in the *F*-region [12]

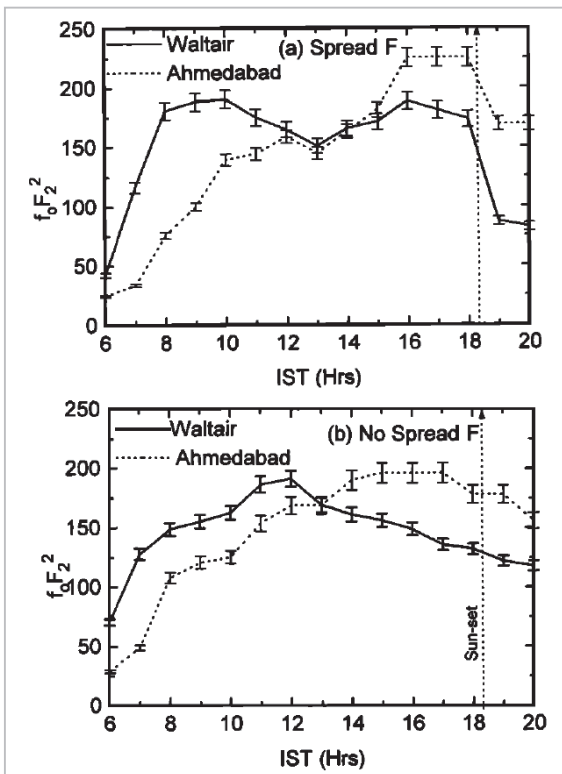


**Fig. 11** Differences in development of the equatorial anomaly immediately before sunset on days when ESF occurs and days when it does not [19]

Local time variation of  $f_oF_2$  as derived from ionosonde observations made at Waltair ( $17.7^\circ\text{N}$ ,  $83.3^\circ\text{E}$ ,  $20.0^\circ\text{N}$  dip latitude), and at Ahmedabad ( $23.0^\circ\text{N}$ ,  $72.4^\circ\text{E}$ ,  $31.5^\circ\text{N}$  dip latitude) in March, April, September and October 1991. Note that the upper panel (a) and lower panel (b) show local time variations of  $f_oF_2$  on days when ESF occurs and days when it does not.

model calculations were performed in considering CEJ, conductivity in the model is based on an empirical model, and the  $\mathbf{E} \times \mathbf{B}$  drift and conductivity calculated in the model are not self-consistent; thus, the two physical processes that connect the EEJ before sunset and PRE as observationally presented here can be considered outside the scope of the model specified in Reference [8]. Therefore, the relationship between the EEJ before sunset and PRE as stated in this paper cannot be verified by the calculation results obtained from Reference [8]. The physical processes between EEJ (including CEJ), PRE and ESF must

therefore be further investigated.

## 4 Conclusion

This paper described the relationship via PRE between EEJ and occurrence of ESF, as clarified by recent observational studies. It was found that a positive correlation does not necessarily exist through all the seasons between the EEJ during the daytime on one hand, and PRE and the occurrence of ESF after sunset on the other, at least in Southeast Asia. It has also been newly clarified that the generation of PRE near sunset and that of ESF after sunset are inhibited through all the seasons when the time integral value of the EEJ strength one to two hours before sunset is negative, in other words, CEJ occurred during the local time immediately before sunset. On the basis that the EEJ before sunset can be observed prior to PRE and the occurrence of ESF, the relationship between the EEJ before sunset on one hand, and PRE and the occurrence of ESF on the other, poses challenges to be further studied to enable the prediction of ESF generation. The physical processes between CEJ immediately before sunset and PRE after sunset have yet to be elucidated. At present, there are at least two conceivable possibilities: a process via a connection of the currents between the EEJ before sunset and the  $F$ -region dynamo near sunset, and a process via changes in the distribution of plasma in the magnetic meridional plane due to the electric field driven by the  $E$ -region dynamo before sunset. To clarify which mechanism is effective, simultaneous observation of PRE and EEJ before sunset at two locations separated by approximately  $15^\circ$  to  $30^\circ$  in longitude, and simultaneous observation of PRE, EEJ and plasma density distribution inside the EIA crests in a meridional plane are required.

## Acknowledgments

The magnetometer data at Kototabang were obtained through joint observations conducted by the Solar-Terrestrial Environment

Laboratory of Nagoya University, the Research Institute for Sustainable Humanosphere of Kyoto University, and Indonesia's National Institute of Aeronautics and Space

(LAPAN). We wish to express our deep appreciation and thanks to those authorities for having provided the data.

## References

- 1 G. Ma and T. Maruyama, "A Storm-Time Super Bubble as Observed with Dense GPS Receiver Network at East Asian Longitudes," Special issue of this NICT Journal, 3-2-9, 2009.
- 2 S. Saito and T. Maruyama, "Effects of Transequatorial Thermospheric Wind on Plasma Bubble Occurrences," Special issue of this NICT Journal, 3-2-2, 2009.
- 3 S. Chapman, "The equatorial electrojet as detected from the abnormal electric current distribution above Huancayo, Peru and elsewhere," *Archiv für Meteorologie, Geophysik und Bioklimatologie*, vol. 44, pp. 368–390, 1951.
- 4 V. Doumouya, J. Vassal, Y. Cohen, O. Fambitakoye, and M. Menvielle, "Equatorial electrojet at African longitudes: first results from magnetic measurements," *Annales Geophysicae*, vol. 16, pp. 658–676, 1998.
- 5 J. A. Bittencourt and M. A. Abdu, "A theoretical comparison between apparent and real vertical ionization drift velocities in the equatorial  $F$  region," *Journal of Geophysical Research*, vol. 86, pp. 2451–2454, 1981.
- 6 B. G. Fejer and L. Scherliess, "Empirical models of storm time equatorial zonal electric fields," *Journal of Geophysical Research*, vol. 102, pp. 24047–24056, 1997.
- 7 B. G. Fejer and L. Scherliess, "On the variability of equatorial  $F$ -region vertical plasma drifts," *Journal of Atmospheric and Solar-Terrestrial Physics*, vol. 63, pp. 893–897, 2001.
- 8 J. V. Eccles, "Modeling investigation of the evening prereversal enhancement of the zonal electric field in the equatorial ionosphere," *Journal of Geophysical Research*, vol. 103, pp. 26709–26719, 1998.
- 9 R. A. Heelis, "Electrodynamics in the low and middle latitude ionosphere: a tutorial," *Journal of Atmospheric and Solar-Terrestrial Physics*, vol. 66, pp. 825–838, 2004.
- 10 H. Rishbeth, "Polarization fields produced by winds in the equatorial  $F$ -region," *Planetary and Space Science*, vol. 19, pp. 357–369, 1971.
- 11 D. T. Farley, E. Bonelli, B. G. Fejer, and M. F. Larsen, "The prereversal enhancement of the zonal electric field in the equatorial ionosphere," *Journal of Geophysical Research*, vol. 91, pp. 13723–13728, 1986.
- 12 G. Haerendel and J. V. Eccles, "The role of the equatorial electrojet in the Evening Ionosphere," *Journal of Geophysical Research*, vol. 97, pp. 1181–1192, 1992.
- 13 P. J. Sultan, "Linear theory and modeling of the Rayleigh-Taylor instability leading to the occurrence of equatorial spread  $F$ ," *Journal of Geophysical Research*, vol. 101, pp. 26875–26891, 1996.
- 14 M. A. Abdu, "Outstanding problems in the equatorial ionosphere?thermosphere electrodynamic relevant to spread  $F$ ," *Journal of Atmospheric and Solar-Terrestrial Physics*, vol. 63, pp. 869–884, 2001.
- 15 R. S. Dabas, Lakha Singh, D. R. Lakshmi, P. Subramanyam, P. Chopra, and S. C. Garg, "Evolution and dynamics of equatorial plasma bubbles: Relationships to  $\mathbf{E} \times \mathbf{B}$  drift, postsunset total electron content enhancements, and equatorial electrojet strength," *Radio Science*, vol. 38, doi: 10.1029/2001RS002586, 2003.

- 
- 16 S. Tulasi Ram, P. V. S. Rama Rao, D. S. V. V. D. Prasad, K. Niranjan, A. Raja Babu, R. Sridharan, C. V. Devasia, and Sudha Ravindran, "The combined effects of electrojet strength and the geomagnetic activity (Kp-index) on the post sunset height rise of the *F*-layer and its role in the generation of ESF during high and low solar activity periods," *Annales Geophysicae*, vol. 25, pp. 2007–2017, 2007.
  - 17 S. Alex and S. Mukherjee, "Local time dependence of the equatorial counter electrojet effect in a narrow longitudinal belt," *Earth Planets Space*, vol. 53, pp. 1151–1161, 2001.
  - 18 C. M. Denardini, M. A. Abdu, E. R. de Paula, C. M. Wrasse, and J. H. A. Sobral, "VHF radar observations of the dip equatorial *E*-region during sunset in the Brazilian sector," *Annales Geophysicae*, vol. 24, pp. 1617–1623, 2006.
  - 19 P. V. S. Rama Rao, P. T. Jayachandran, and P. Sri Ram, "Ionospheric irregularities-role of Equatorial Ionization Anomaly," *Radio Science*, vol. 32, pp. 1551–1556, 1997.
  - 20 S. V. Thampi, S. Ravindran, T. K. Pant, C. V. Devasia, and R. Sridharan, "Seasonal dependence of the "forecast parameter" based on the EIA characteristics for the prediction of Equatorial Spread F (ESF)," *Annales Geophysicae*, vol. 26, pp. 1751–1757, 2008.
  - 21 S. Prakash, D. Pallamraju, and H. S. S. Sinha, "Role of the equatorial ionization anomaly in the development of the evening prereversal enhancement of the equatorial zonal electric field," *Journal of Geophysical Research*, vol. 114, A02301, doi: 10.1029/2007JA012808, 2009.

---

**UEMOTO Jyunpei, Ph.D.**

*Expert Researcher, Space Environment  
Group, Applied Electromagnetic  
Research Center*

*Aeronomy*

---

**MARUYAMA Takashi, Ph.D. (Eng.)**

*Executive Researcher  
Upper Atmospheric Physics*



**SAITO Susumu, Ph.D.**

*Senior Researcher, Communication,  
Navigation, and Surveillance  
Department, Electronic Navigation  
Research Institute*

*Aeronomy, Satellite Navigation*

**ISHII Mamoru, Dr. Sci.**

*Director, Project Promotion Office,  
Applied Electromagnetic Research  
Center*

*Upper Atmospheric Physics*

**YOSHIMURA Reiko, Ph.D.**

*Instructor, Center for Natural Science,  
Kitasato University*

*Aeronomy*